Journal of Molecular Liquids 301 (2020) 112433

Contents lists available at ScienceDirect

Journal of Molecular Liquids

journal homepage: www.elsevier.com/locate/molliq

Aqueous sorption of tetracycline using rarasaponin-modified nanocrystalline cellulose

Vania Bundjaja [a], Tirta Mutiara Sari [a], Felycia Edi Soetaredjo [a,b], Maria Yuliana [a], Artik Elisa Angkawijaya [c], Suryadi Ismadji [a,b], Kuan-Chen Cheng [d,e,f], Shella Permatasari Santoso [a,b,*]

[a] Department of Chemical Engineering, Widya Mandala Surabaya Catholic University, Surabaya 60114, Indonesia
[b] Chemical Engineering Department, National Taiwan University of Science and Technology, Taipei 106, Taiwan
[c] Graduate Institute of Applied Science and Technology, National Taiwan University of Science and Technology, Taipei 106, Taiwan
[d] Institute of Biotechnology, National Taiwan University, No. 1, Sec. 4, Roosevelt Rd., Taipei 10617, Taiwan
[e] Graduate Institute of Food Science and Technology, National Taiwan University, No. 1, Sec. 4, Roosevelt Rd., Taipei 10617, Taiwan
[f] Department of Medical Research, China Medical University Hospital, China Medical University, No. 91, Hsueh-Shih Rd., Taichung 40402, Taiwan

ARTICLE INFO

Article history:
Received 7 October 2019
Received in revised form 27 December 2019
Accepted 31 December 2019
Available online xxxx

Keywords:
Cellulose
Nanocrystal
Rarasaponin
Surface modification
Tetracycline
Drug delivery

ABSTRACT

The sorption ability of NCC and its modified form against tetracycline were investigated. NCC modification was carried out using a natural surfactant, namely rarasaponin, to improve the NCC adsorption capacity. The modification was made with a mass ratio of NCC to rarasaponin 10:1 (10N1R) and 20:1 (20N1R). The modified NCC characteristics were investigated using Fourier transform infrared (FTIR), zeta potential analyzer, X-ray diffraction (XRD), and scanning electron microscope (SEM). There are no structural changes to the surfactant-modified NCC, as revealed by SEM. However, other characterizations show that the incorporation of rarasaponin indeed altered some characteristics of NCC. The modified NCC shows higher adsorption capacity towards TET. The adsorption capacity of TET was 13.97, 16.47, and 18.11 mg/g (at 60 °C) for NCC, 10N1R, and 20N1R, respectively. The kinetic release (desorption) study of TET@20N1R showed a release efficiency of 18.28% at pH 3 and 55.49% at pH 7.

1. Introduction

The use of nanoparticles for applications in the medical field, such as drug carriers, has been widely anticipated. Many studies have shown that modification of particle size to nano can improve material compatibility. In addition, nanoparticles have superior characteristics such as high surface to mass ratio, good adsorption ability, modifiable selectivity, and easy degradation. Over the years, various synthetic polymers such as poly(lactic-*co*-glycolic acid) (PLGA), poly(ε-caprolactone), poly(ethylene glycol) (PEG), and poly(N-(2-hydroxypropyl) methacrylamide) (PLG), has been widely used to prepare nano-sized drug carriers [1]. The use of synthetic polymers has several limitations, especially in their high immunogenicity, which causes adverse effects on their long-term use [2,3]. For this reason, the use of natural polymers such as chitosan, alginate, collagen, and cellulose, for the synthesis of drug carriers has received much attention [4].

Nanocrystalline cellulose (NCC) is a nano-sized particle derived from a natural polymer, cellulose, whose modification has been extensively studied. The vast interest in NCC is due to its high biocompatibility, which is assisted by other superior properties, such as abundantly available, natural, and non-toxic. Structurally, the surface of NCC is rich in hydroxyl groups, which provide modification sites for many functional applications. Surface modification of NCC is a common practice of cellulose modification for the preparation of drug-carriers and other advanced materials [5–11]. Some surface modification techniques available are esterification, cationization, sulfonation, oxidation, silylation, esterification, functional compound or polymer grafting, and carboxylation. Surface modification of NCC by incorporating functional compound is widely performed among the available techniques. This is because other modification techniques (e.g., oxidation) often alter the structure of the NCC, which can result in decreased surface area, structural stability, and mechanical strength [8–10].

In this study, we investigated the effects of a natural surfactant (i.e., rarasaponin, as a surface modifying agent) on the ability of NCC as a drug loading and releasing the device. Rarasaponin is extracted from *Sapindus rarak DC*; so far, it has been used as a modifying agent

* Corresponding author at: Department of Chemical Engineering, Widya Mandala Surabaya Catholic University, Surabaya 60114, Indonesia.
E-mail address: shella_p5@yahoo.com (S.P. Santoso).

https://doi.org/10.1016/j.molliq.2019.112433
0167-7322/

for clay materials to remove various hazardous substances from water or wastewater. The results show that the incorporation of rarasaponin into clay can significantly increase the adsorption capacity of clay [12–14]. Here, rarasaponin is incorporated with NCC before improving the drug adsorption capacity, which yet to be done to date. Modification of NCC with surfactants (other than rarasaponin) has been carried out [7,15,16]. For instance, Jackson and co-researchers used cetyltrimethylammonium bromide (CTAB) to modify NCC; they reported that only ~6% (from 100 μg) paclitaxel drug could be loaded onto 2 mg of unmodified NCC, while up to ~85% paclitaxel could be loaded onto 2 mg of NCC modified with 12.9 mM CTAB [7]. Natural surfactant (i.e., rarasaponin) was chosen since natural surfactants are environmentally friendly materials that are generally more easily degraded, less toxic, and also easily digested; compared to synthetic surfactants [17].

Tetracycline is a widely used antibiotic that works against gram-positive and gram-negative bacteria. It has three ionizable functional groups that can undergo protonation/deprotonation depending on the pH of the solution (Fig. S1) [18,19]. The main challenge for tetracycline administration is to increase drug bioavailability [20]. Antibiotic drug delivery system is essential for eradicating microorganisms associated with bacterial infections and causing lower doses, toxicity reduction, extended-release, and minimizing systemic exposure [21]. The loading capacity of rarasaponin-modified NCC was investigated by means of adsorption studies on tetracycline drugs. Drug desorption kinetics were also performed and modeled.

2. Materials and methods

2.1. Materials

Analytical grade sulfuric acid (H_2SO_4, 95–98% purity), sodium hydroxide (NaOH, ≥97% purity), disodium hydrogen phosphate (Na_2HPO_4, ≥99% purity), potassium dihydrogen phosphate (KH_2PO_4, ≥99% purity), phosphoric acid (H_3PO_4, 85 wt% in H_2O), sodium chloride (NaCl, ≥99% purity), and tetracycline ($C_{22}H_{24}N_2O_8$, ≥98% purity) were purchased from Sigma-Aldrich (Singapore). *Sapindus rarak DC* fruits were obtained from Malang, East Java, Indonesia. Reversed osmosis (RO) water was used in this study to dissolve chemicals and treat samples. Dialysis membrane tubes (MWCO 12–14 kD) were purchased from Spectrum Laboratories, Inc.

2.2. Preparation of cellulose nanocrystals

NCC was prepared from filter paper (Whatman #1) through the hydrolysis process using concentrated sulfuric acid [9,22]. Briefly, 10 g filter paper was soaked in 87.5 mL of H_2SO_4 solution (64 wt%). The hydrolysis was carried out for 1 h at 45 °C with constant stirring. Substantial amounts of cold water were then added to stop hydrolysis; two layers (suspension layer and clear layer) were then formed. The cloudy suspension layer was collected and then centrifuged at 10,000 rpm for 10 min. The centrifuged solids were then put into a dialysis tube against RO water; the water was continuously changed until the pH of the dialysate reached 6. The neutralized suspension was then ultra-sonicated for 30 min and kept at −40 °C before freeze-drying.

2.3. Rarasaponin extraction

Rarasaponin was extracted from the *Sapindus rarak* DC fruits according to a previously reported method [13]. Briefly, dried-fruit seeds were removed from pericarps. Subsequently, the pericarps were pulverized to obtain powdered fruit. 50 g of fruit powder extracted with 500 mL of distilled water, at 80 °C for 1 h with constant stirring. The rarasaponin extract was separated from the solid residue using centrifugation at 4000 rpm for 10 min. The rarasaponin dry extract was obtained by oven drying at 80 °C, followed by air drying for 24 h. The extracted rarasaponin was quantified for its saponin content using a sulfuric-vanillin reagent according to the method reported by Hiai and groups [23]. The total saponin content of the extracted rarasaponin was 18.82 ± 0.19% from dry fruit weight.

2.4. Surface modification of NCC

The surface modification of NCC was carried out under different NCC-to-rarasaponin mass ratios (10:1 and 20:1). For simplicity purposes, samples were denoted as 10N1R and 20N1R for a sample of the NCC-to-rarasaponin ratio of 10 and 20, respectively. 10N1R was prepared by slowly adding 1 g NCC suspension (in 100 mL RO water) to 0.1 g rarasaponin in 100 mL RO water. The mixture was heated at 45 °C for 1 h under constant stirring. The unbound rarasaponin was separated using a centrifuge that operates at 10,000 rpm for 10 min. The resulting NCC-rarasaponin (NCC/Rara) was dried in a freeze dryer. The same procedure was used to prepare 20N1R, except the rarasaponin solution, was prepared by dissolving 0.05 g of rarasaponin in 100 mL of RO water.

2.5. Characterization

The surface functional groups were determined using Fourier Transform Infrared (FTIR) analysis using a Shimadzu 8400S; the KBr pellet was used as the background, and the measurements were conducted at wavenumber range of 4000–400 cm^{-1}. Zeta Potential analyzer (Brookhaven 90Plus) was employed to measure the surface charge of the samples (0.01%wt in deionized water) at various pHs. X-ray diffraction (XRD) patterns were recorded at 40 kV and 30 mA using a Rigaku Miniflex Goniometer with Cu Kα radiation, while the surface topography was acquired using surface electron microscopy analysis on a JEOL JSM-6500F with Pt coating and 5.0 kV acceleration voltage. A Java-based image processing and analysis program, namely ImageJ, was used to determine the dimension of the NCC and NCC/Rara crystal particles.

2.6. Adsorption study

Tetracycline (TET) adsorption was studied isothermally at various temperatures (30, 45, and 60 °C). The TET adsorbate was prepared at a concentration of 100 ppm in phosphate buffer at pH 3. The choice of pH was based on the previous study by Wijaya et al. which shows that the adsorption capacity at pH 3 was the highest; this is since TET present as cations at pH < 3.3 [24]. Various NCC masses (10–20 mg) were then introduced in closed-dark-flasks containing 10 mL of prepared TET solution. The flasks were put in a thermostatic shaking water bath (Memmert type WB-14) and operated at 200 rpm for 8 h. Subsequently, the suspension was separated by centrifugation. The unadsorbed (unloaded) TET was measured using a spectrophotometer at an optical density of 610 nm (OD_{610}). The amount of TET adsorbed (loaded) on NCC was calculated according to Eq. (1):

$$q_e = \frac{C_0 - C_e}{m} \times V \quad (1)$$

where q_e is the amount of TET adsorbed per g of adsorbent, C_0, and C_e (mg/L) are the initial and residual concentration of TET, respectively. V (L) is the total volume of the investigated system, and m (g) is the mass of NCC added.

The kinetic adsorption of TET onto NCC or NCC/Rara was studied at a pH of 3 and a temperature of 30 °C. 20 mg of adsorbent was suspended in 10 mL of 100 ppm TET solution and then shaken in a thermostatic shaking water bath at 200 rpm. The concentration of residual TET was measured at a certain interval of time. The amount

of TET adsorbed at a certain time interval was calculated by using Eq. (2):

$$q_t = \frac{C_0 - C_t}{m} \times V \quad (2)$$

where q_t (mg/g) is the uptake of TET at time t, and C_t (mg/L) is the concentration of TET at time *t*.

2.7. Release kinetic study

The *in vitro* drug release experiments were performed at 37 °C in a phosphate-buffered solution. The study was conducted at pH 3 and 7 to mimic the pH of gastric acid in the human stomach lumen and body fluid, respectively. A release study was conducted on a drug carrier (sample) that provided the highest amount of TET loaded. Drug release was carried out by suspending 20 mg of freeze-dried TET-loaded NCC/Rara (TET@NCC/Rara) in 10 mL of phosphate buffer. The suspensions were placed in a thermostatic shaker water bath and shaken at 200 rpm. At a specific interval time, the tube was taken and centrifuged. The concentration of released drug was determined by using a spectrophotometer at OD_{610}.

3. Result and discussion

3.1. Preparation of NCC-rarasaponin (NCC/Rara)

3.1.1. The formation mechanism of NCC/Rara

Nano-sized cellulose crystals (NCC) were obtained from the hydrolysis of cellulose using sulfuric acid. The formed NCC crystals contain abundant hydroxyl (OH) groups and approximately 1 sulfate ester group in each 6 OH groups [9,25]. The OH group in the sixth position is the primary alcohol in which the modifications occur [26]. The incorporation of rarasaponin then occurs via hydrogen bonds [27]. The intermolecular hydrogen bonds involve the oxygen atom at the carboxyl group of rarasaponin (partial negative charge) and hydrogen atom at OH group of NCC (partial positive charge). The overall formation mechanism of NCC/Rara is depicted in Fig. 1.

3.1.2. Characterization of NCC/Rara

The NCC/Rara was prepared at two different NCC-to-rarasaponin mass ratio, that is 10N1R and 20N1R. Several characterizations such as FTIR, Zeta potential, XRD, and SEM were conducted to characterize samples (rarasaponin, NCC, 10N1R, and 20N1R).

Surface functional groups of rarasaponin, NCC, and NCC/Rara were determined using FTIR analysis, and the results are presented in the Supplementary data Fig. S2 and Table S1. A broad absorption peak was observed at 3310–3269 cm^{-1}, which refers to OH stretching; this was observed in all samples. Meanwhile, the bending vibration of OH due to the relationship of water molecules was observed at 1632–1611 cm^{-1}. A peak at 1254–1244 cm^{-1}, indicating the presence of sulfonate groups, was noted for NCC and NCC/Rara. The addition of rarasaponin induces changes in several NCC absorption peaks. For instance, the absorption peak which corresponds to OH stretching was appeared at a lower frequency in NCC/Rara (3275–3171 cm^{-1}) compared to NCC (3277 cm^{-1}); this suggests the involvement of the OH group in the formation of NCC/Rara. The shifting to the lower frequency is due to the disappearance of some of OH groups [28] as they bounded with rarasaponin. The peak corresponding to C═C stretching appeared only in rarasaponin (1685 cm^{-1}), and NCC/Rara (1694–1695 cm^{-1}), indicates the presence of rarasaponin in NCC/Rara.

The zeta potential values of the NCC and NCC/Rara were shown in Fig. S3. In the pH range of 2 to 10, a negative surface charge of NCC with a net surface charge of −6 to −8 mV was observed. Incorporation of rarasaponin causes the net surface charge of NCC to be more negative; that is −8 to −11 mV for 10N1R and − 11 to −14 mV for 20N1R. The increase in surface charge negativity is caused by the presence of deacylated carbonyl groups originating from rarasaponin. Putro and coworkers also observed a similar phenomenon in the decrease of net surface charge (becoming more negative) due to the modification of NCC using anionic surfactants. The zeta potential of NCC decreased from −25.24 to −37.92 mV after modification with anionic SDS [15].

The XRD patterns of NCC and NCC/Rara were given in Fig. S4. It can be seen that all samples possess major peaks at $2\theta = 15°$, 16.5°, and 22°, which respectively represent 101, 10$\bar{1}$, and 002 planes. The XRD pattern of NCC/Rara shows no significant difference compared to NCC. The crystallinity index (CrI) of the samples was calculated from the published equation [29]; the detailed calculations were provided in

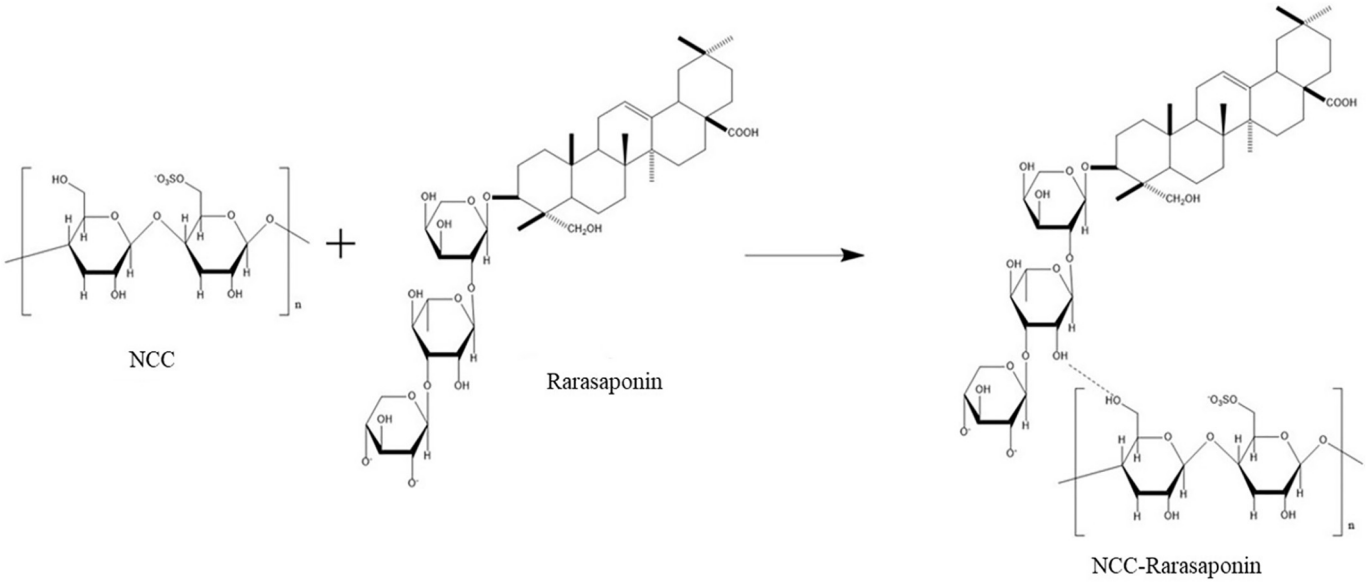

Fig. 1. The proposed formation mechanism of NCC/Rara.

Supplementary data Table S2. CrI of 74.6, 70.9, and 71.2% were obtained for NCC, 10N1R, and 20N1R, respectively. The crystallinity of NCC/Rara was found to be slightly lower than NCC. The intensity of the 002 plane for NCC/Rara was smaller than NCC itself; but, the intensity at 101 and 10ī planes was greater for NCC/Rara. The decrease in CrI is due to the incorporation of the non-crystalline rarasaponin [9,15,30].

SEM analysis was carried out to observe the morphological of NCC and NCC/Rara. The SEM image (Supplementary data Fig. S5) shows a rod-like crystal structure of NCC. The estimation on crystals dimensions using ImageJ shows that the synthesized NCC have a particle length of 237.4 ± 52.0 nm, and particle width of 29.9 ± 5.9 nm. Surface modification of NCC using rarasaponin does not cause any alteration in the morphological appearance of NCC. However, the dimension analysis shows that the incorporation of rarasaponin produced larger particle sizes. The NCC/Rara has a particle length of 356.3 ± 60.7 nm and a width of 52.3 ± 8.2 nm.

3.2. Adsorption mechanism of TET on NCC/Rara

NCC/Rara contains unoccupied sulfate ester sites and deacylated carbonyl sites, as shown in Fig. 1. These active sites play an essential role in attracting TET molecules. In Fig. 2, the illustration of TET loading onto 10N1R (higher rarasaponin concentration) and 20N1R (lower rarasaponin concentration) are shown. Attachment of cationic TET onto 10N1R or 20N1R induced by electrostatic interactions [9,15,19]; that is between the positively charged amide group of TET against sulfate ester and the deacylated carbonyl group of NCC/Rara. Based on the phenomena observed in the adsorption study (discussed in the next section) and the concentration of rarasaponin, we proposed two different mechanisms of TET loading onto NCC/Rara:

(I) At high rarasaponin concentration, TET@10N1R. In this case, the number of rarasaponin molecules is over-numbered NCC; thus, some rarasaponin molecules cannot be successfully bound to NCC particles. Furthermore, the unbounded rarasaponin molecules interact to form micelles. Later on, these micelles cause interference with the adsorption of TET onto 10N1R, thereby reducing adsorption efficiency.

(II) At low rarasaponin concentration, TET@20N1R. In this case, the number of NCC particles is sufficient to accommodate rarasaponin molecules; thus, the formation of micelles is minimized, thereby more TET molecules can be loaded onto the adsorbent.

3.3. Adsorption isotherm study

In the present study, Langmuir and Freundlich were fitted to the experimental data to understand the interactions between adsorbate and adsorbents [30–32]. The Langmuir model is mathematically expressed as Eq. (3):

$$q_e = q_{max}\frac{K_L C_e}{1 + K_L C_e} \tag{3}$$

where q_e is milligrams of TET adsorbed per grams of adsorbent, C_e is milligrams of residual TET per liter of solution at equilibrium, K_L is the Langmuir affinity constant in units of (L/mg), and q_{max} is the maximum adsorption capacity of the adsorbent with monolayer surface coverage in units of (mg/g) [31].

Freundlich equilibrium isotherm is used to describe the multilayer adsorption with the interaction between adsorbed molecules. Freundlich model is represented in mathematics forms as Eq. (4):

$$q_e = K_F C_e^{1/n} \tag{4}$$

where K_F is the measure of Freundlich adsorption capacity in units of $(mg/g)(L/mg)^{-1/n}$ and $1/n$ is a heterogeneity factor that has no units (dimensionless). For favorable adsorption, the value of n must fall between 1 and 10 [33].

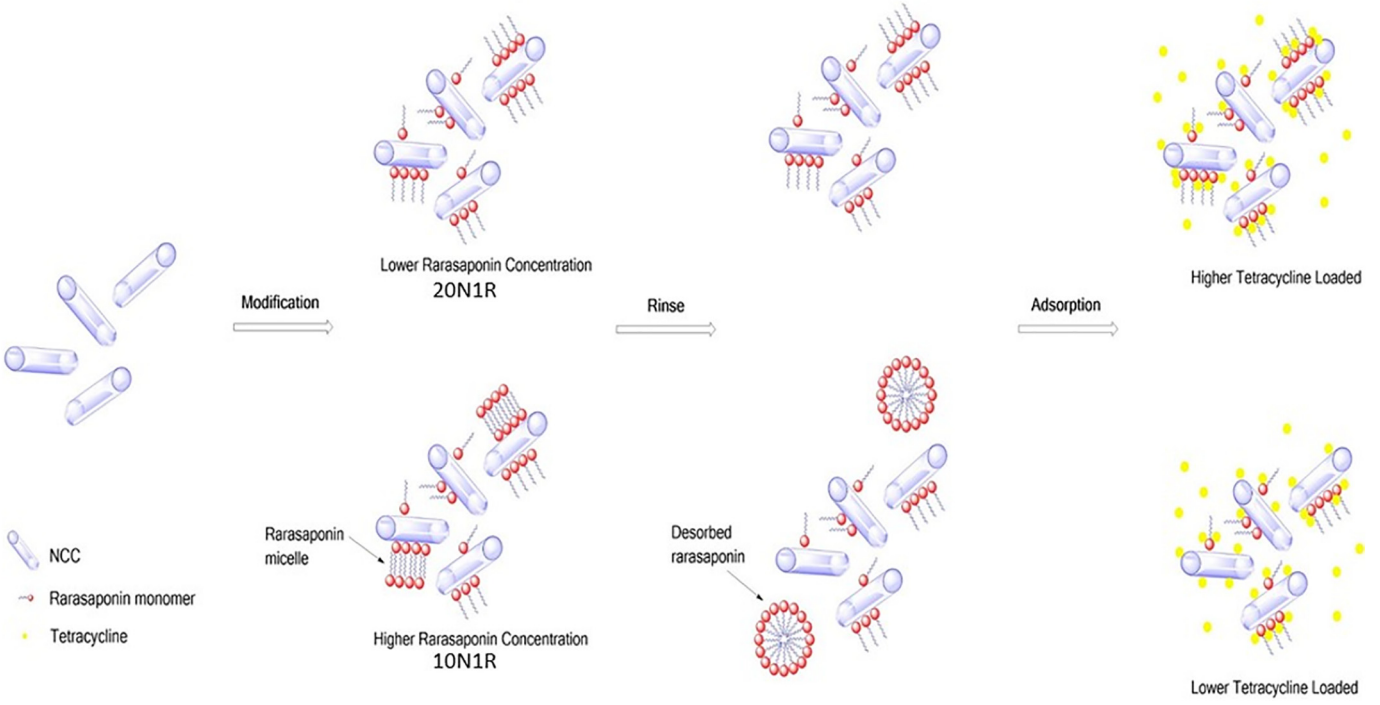

Fig. 2. Illustration of adsorption of TET@10N1R and TET@20N1R. Impurities (e.g., sugars, alkaloid, and phenolic) from the rarasaponin-crude-extract were not illustrated for simplification purposes.

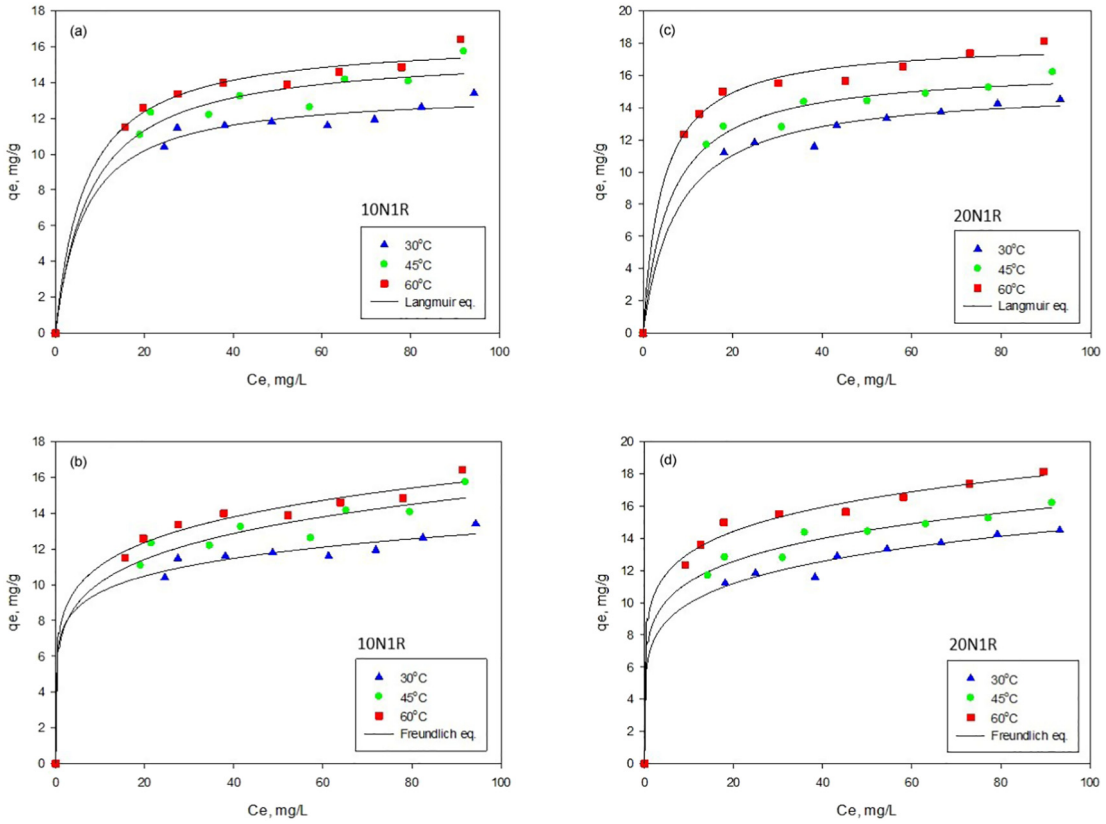

Fig. 3. Adsorption isotherms of TET@10N1R (a, b), TET@20N1R (c, d) with Langmuir and Freundlich fittings.

The adsorption isotherm profile of TET@NCC is presented in the Supplementary data Fig. S6, while TET@10N1R and TET@20N1R are shown in Fig. 3. The parameters of the two models are summarized in Table 1. The adsorption mechanism can be studied from the adsorption isotherm model. Langmuir isotherm assumes a monolayer coverage on a homogeneous surface with a particular adsorption site, while Freundlich isotherm assumes that the adsorbates form a multilayer with interactions between the adsorbed molecules [34].

Both models can predict well the maximum adsorption capacity of TET onto the adsorbent under study. Based on the value of the correlation coefficient (R^2), it was found that the Freundlich equation gives a slightly better fitting than the Langmuir equation for all adsorbent systems. This indicates that the adsorption occurs on the non-homogeneous surface of adsorbents. The arise of in-homogeneity is due to the random charge distribution and uneven distribution of rarasaponin on the adsorbent surface. The calculated maximum adsorption capacity (q_{max}) indicates that 20N1R can adsorb more TET, followed by 10N1R and NCC; it suggests that the addition of rarasaponin provides more adsorption active sites. The higher adsorption capacity of 20N1R than 10N1R is influenced by the activity of rarasaponin, as illustrated in Fig. 2. Higher rarasaponin concentration, in 10N1R, causes a decrease in adsorption. In 10N1R, the excess rarasaponin molecules tend to form surfactant aggregations called micelles. These micelles interfere with the interaction between adsorbate and adsorbent; the micelles capture TET molecules and keep them hovering in solution so that the adsorption capacity of the adsorbate decreased. While at 20N1R, there are enough NCC particles to accommodate the rarasaponin molecule on its surface; thus, rarasaponin can act as hands which helps in capturing TET molecules and supports adsorption. This argument also supported by the measured surface charge by zeta potential analyzer. 20N1R sample shows a more negative surface charge than 10N1R; indicates that the more considerable amount of rarasaponin is attached on its surface than on 10N1R. Rarasaponin itself has a negative zeta potential, that is −3 so that the presence of rarasaponin contributes to the more negative zeta potential of the samples. The effect of temperature was also investigated in the adsorption isotherm. The increase in temperature promotes the uptake of TET onto the adsorbents. This indicates that the adsorption of TET onto NCC, 10N1R, and 20N1R is endothermic.

Table 1
The parameters of Langmuir and Freundlich models for the adsorption system of TET onto NCC, 10N1R, and 20N1R.

T (°C)	Langmuir			Freundlich		
	K_L (L/mg)	q_{max} (mg/g)	R^2	K_F (mg/g)(L/mg)$^{-1/n}$	n	R^2
TET@NCC						
30	0.0102	11.9440	0.9933	0.5033	1.8529	0.9941
45	0.0175	11.2567	0.9803	1.0104	2.3446	0.9826
60	0.0175	13.9675	0.9910	1.1830	2.2746	0.9921
TET@10N1R						
30	0.1523	13.5289	0.9880	7.0921	7.6631	0.9902
45	0.1285	15.7013	0.9756	6.8120	5.8041	0.9825
60	0.1503	16.4692	0.9896	7.6764	6.2946	0.9921
TET@20N1R						
30	0.1307	15.2738	0.9885	6.7777	5.9770	0.9940
45	0.1660	16.4783	0.9896	7.9055	6.4674	0.9936
60	0.2339	18.1089	0.9916	9.3992	6.9949	0.9938

3.4. Adsorption kinetic study

Adsorption kinetic is the rate of adsorbate adsorbed onto the surface of the adsorbent. Several kinetic models are available to represent the adsorption kinetic data, such as pseudo-first-order and pseudo-

second-order. Both models are the most commonly used models to predict the behavior of the liquid phase adsorption. The mathematical form of the pseudo-first-order kinetic can be expressed as:

$$\frac{dq_t}{dt} = k_1(q_e - q_t) \tag{5}$$

By integrating the equation above, the final form of pseudo-first-order is:

$$q_t = q_e\left[1-\left(e^{-k_1 t}\right)\right] \tag{6}$$

where q_t and q_e are milligrams of TET adsorbed per grams of adsorbent at time t (min) and at equilibrium respectively, and k_1 is the rate constant of the pseudo-first-order fitting in units of (min^{-1}).

While the mathematical form of the pseudo-second-order kinetic can be expressed as:

$$\frac{dq_t}{dt} = k_2(q_e - q_t)^2 \tag{7}$$

By integrating the equation above, the final form of pseudo-second-order is:

$$q_t = q_e\left(\frac{q_e k_2 t}{1 + q_e k_2 t}\right) \tag{8}$$

where k_2 is the rate constant of pseudo-second-order adsorption fitting in units of (g/mg·min). k_1 and k_2 parameters show time needed by the system to reach the equilibrium [35,36].

As shown in Fig. 4, each kinetic adsorption system reaches equilibrium in approximately 360 min. A plateau was observed afterward. The parameters obtained from the pseudo-first and pseudo-second-order fittings are given in Table 2. Based on the correlation coefficient (R^2), the two equations can represent the adsorption kinetics of TET antibiotic onto NCC, 10N1R, and 20N1R quite well. However, based on the q_t values, it is convinced that pseudo-first-order can predict adsorption capacity better than pseudo-second-order. The q_t obtained from pseudo-first-order is closer to the adsorption capacity of the experiment. The pseudo-first-order model assumes that physisorption controls the adsorption process more than chemisorption — the time scaling parameter k_1 and k_2 in pseudo-first and pseudo-second-order measure the time needed to reach equilibrium. The time scaling parameter is reduced on surfactant-modified NCC, and the time required to achieve the equilibrium condition is longer.

Table 2
Parameter of pseudo-first order and pseudo-second-order for TET adsorption onto NCC, 10N1R, and 20N1R.

Adsorbents	Pseudo first order			Pseudo second order		
	k_1 (min^{-1})	q_e (mg/g)	R^2	k_2 (g/mg·min^{-1})	q_e (mg/g)	R^2
NCC	0.0122	6.4020	0.9825	0.0014	8.1763	0.9747
10N1R	0.0109	9.6084	0.9631	0.0008	12.3850	0.9607
20N1R	0.0107	12.1760	0.9851	0.0006	16.0689	0.9806

3.5. A comparison study on the loading capacity of surfactant-modified NCC

The addition of surfactants can provide additional active sites that promote the adsorption of adsorbate molecules that are dispersed in bulk solution. The enhancement of drug loading capacity by surfactant-modified NCC has been proven in some studies. Some of the studies are summarized in Table 3. It can be seen that the surfactant-modified NCC has a higher drug loading capacity; for instance, only ~6 μg Docetaxel can be loaded on 1 mg of unmodified NCC, and ~40.5 μg Docetaxel can be loaded on 1 mg of CTAB-modified NCC [7]. Putro and group also showed that CTAB-modified NCC could load Paclitaxel 50-times higher than the unmodified NCC. In this work, the addition of rarasaponin also gives an enhancement in the loading capacity of TET, which is 1.12-times and 1.30-times higher for 10N1R and 20N1R, respectively.

The enhancement in loading capacity provided by rarasaponin is much lower compared to CTAB, SDS, or Tween 20. This is because the extracted rarasaponin from *Sapindus rarak* still contains other crude compounds (impurities), other than rarasaponins, which is typical for many plant extracts [37,38]. As mentioned by Karim = and Azlan, *Sapindus rarak* pericarp contains many bioactive compounds such as raraoside, rarasaponin, saponins, acyclic sesquiterpene glycosides, and hederagenin [39]. A qualitative study of *Sapindus rarak* water extract showed positive results for the presence of compounds other than rarasaponin, namely flavonoids, alkaloids, tannins, and polyphenols [39,40]. The presence of impurities can interfere with the interaction of TET molecules with rarasaponin and NCC. Nevertheless, rarasaponin as a natural surfactant can be more beneficial, especially in terms of environmental friendliness. In the term of biocompatibility, it should be noted that surfactant induced cytotoxicity in healthy cells if used at a high concentration. As demonstrated by Putro et al., good biocompatibility is still maintained at Tween 20 concentration of 10 μg/mL, where Tween 20 only induces ~15% 7F2-cells (mouse osteoblast cells) death after 24 h; while at concentrations higher than 25 μg/mL, ~25%

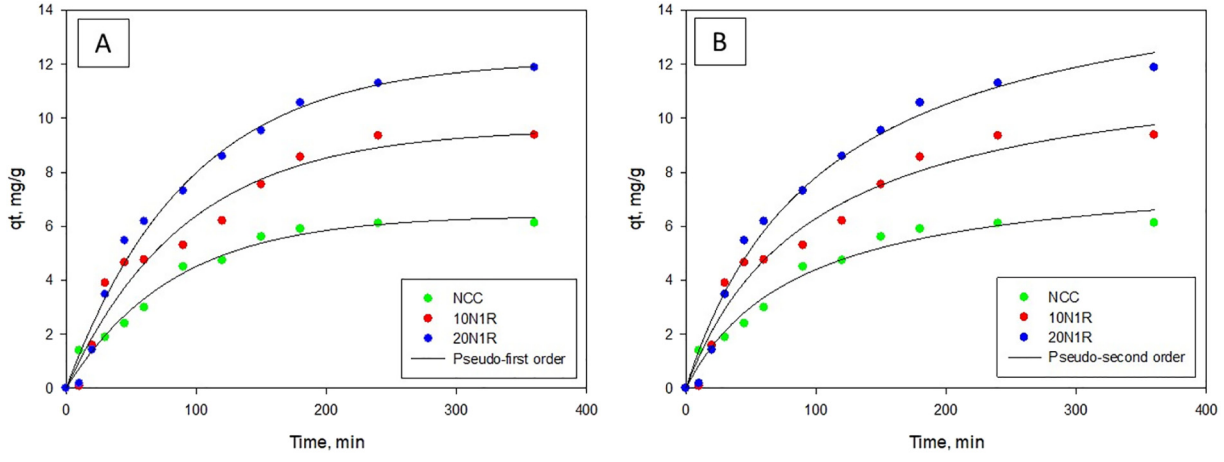

Fig. 4. Adsorption kinetics of TET onto NCC, 10N1R, and 20N1R with (A) pseudo-first-order fitting and (B) pseudo-second-order fitting.

Table 3
Comparison of drug loading capacity on unmodified and surfactant modified NCC.

Modifying agent		Drug	Drug loaded (μg/mg)		Ref
Comp.[a]	Conc.		Unmodified	Modified	
CTAB	12.9 mM	Docetaxel	6[b]	40.5[b]	[7]
		Paclitaxel	3.5[b]	42[b]	
		Etoposide	1.3[b]	25[b]	
CTAB	15 mM	Paclitaxel	1.3[b]	65.5	[15]
SDS			1.2[b]	41[b]	
Tween 20			1.3[b]	28[b]	
CTAB	0.4 g/L	Luteolin	–	12.9	[16]
		Luteoloside	–	56.9	
Rarasaponin	0.5–1 g/L	Tetracycline	13.97	16.47 (10N1R) 18.11 (20N1R)	This study

[a] CTAB = cetyltrimethylammonium bromide, SDS = sodium dodecyl sulfate.
[b] Approximated value based on the presented graphical (curve) data in the literature.

Table 4
Thermodynamic parameters of TET adsorption onto NCC, 10N1R, and 20N1R.

Adsorbents	$\Delta G°$ (kJ/mol)			$\Delta H°$ (kJ/mol)	$\Delta S°$ (J/mol·K)
	30 °C	45 °C	60 °C		
NCC	5.20	4.76	3.28	24.41	62.88
10N1R	−8.69	−6.58	−10.17	5.36	43.51
20N1R	−8.23	−10.55	−13.68	46.65	180.71

cell death is observed. In this study, the rarasaponin extract used was much lower (0.5–1 μg/mL) so that good biocompatibility could still be expected [15]. Moreover, Morikawa and co-researchers also show that purified *Sapindus rarak* extract (30–100 mM) has good biological activity, which is induced cytotoxicity on tumor necrosis in L929 cells [41]. A study by Faysoon also noted that *Sapindus rarak* extract induces moderate cytotoxicity against human gastric carcinoma, with IC50 values of 5.55 μg/mL [42].

3.6. Thermodynamic parameters of the adsorption

The thermodynamic parameters, including the changes in the standard Gibbs free energy ($\Delta G°$), enthalpy ($\Delta H°$), and entropy ($\Delta S°$) were calculated by Eqs. (9) and (10):

$$\Delta G^\circ = -RT\ \ln K_D \tag{9}$$

$$\ln K_D = -\frac{\Delta H^\circ}{RT} + \frac{\Delta S^\circ}{R} \tag{10}$$

Table 5
Parameters of pseudo-first order and pseudo-second order of TET@20N1R desorption.

pH	Pseudo-first order		
	k_{1D} (min^{-1})	q_{eD} (mg/g)	R^2
3	0.1075	3.0377	0.9078
7	0.1597	7.7903	0.9673
pH	Pseudo-second order		
	k_{2D} (min^{-1})	q_{eD} (mg/g)	R^2
3	0.0134	4.9699	0.9014
7	0.0105	11.3466	0.9589

where R is the universal gas constant (8.314 J/mol·K), T is the temperature in units of (K), and K_D is the distribution coefficient. Values of ln K_D were determined from the regression of ln (q_e/C_e) versus q_e. Subsequently, the plotting of ln K_D versus 1/T (as shown in Supplementary data Fig. S7) gives the value of $\Delta H°$ (slope) and $\Delta S°$ (intercept) [43,44]. The calculated thermodynamic parameters are listed in Table 4.

A positive $\Delta G°$ value of adsorption of TET@NCC implies a non-spontaneous process. Meanwhile, a negative $\Delta G°$ value was observed for adsorption of TET@10N1R and TET@20N1R. This suggests that the addition of rarasaponin provides additional active sites that promote spontaneous adsorption. Positive values of $\Delta H°$ confirm the endothermic nature of the adsorption [45]. Positive $\Delta S°$ values for all adsorbent indicates that there was an increase in the randomness of the solid-solution interface during adsorption. The positive $\Delta S°$ also suggests that the adsorption process is irreversible in the current adsorption pH, media, and temperature.

3.7. Desorption kinetic study

The desorption kinetic study was performed for TET@20N1R since this system has the highest TET loading. The desorption of TET@20N1R was investigated in phosphate buffer medium at pH of 3 and 7; the rate of desorption was modeled using the pseudo-first-order and pseudo-second-order model. As shown in Fig. 5, the TET desorption profile of 20N1R differs at pH 3 and pH 7. This indicates that the release of TET is pH-dependent. The release of TET continues, and the plateau was achieved after 14 h. The parameters resulting from the fitting of desorption kinetics are summarized in Table 5, where q_{eD} shows the amount of TET released at equilibrium time per mass of adsorbent. The desorption efficiency is determined by dividing the amount of desorbed TET with the amount of initial TET.

The desorption efficiency at pH 3 is found to be 18.28%, which is lower than the desorption efficiency at pH 7, which is 55.49%. This is

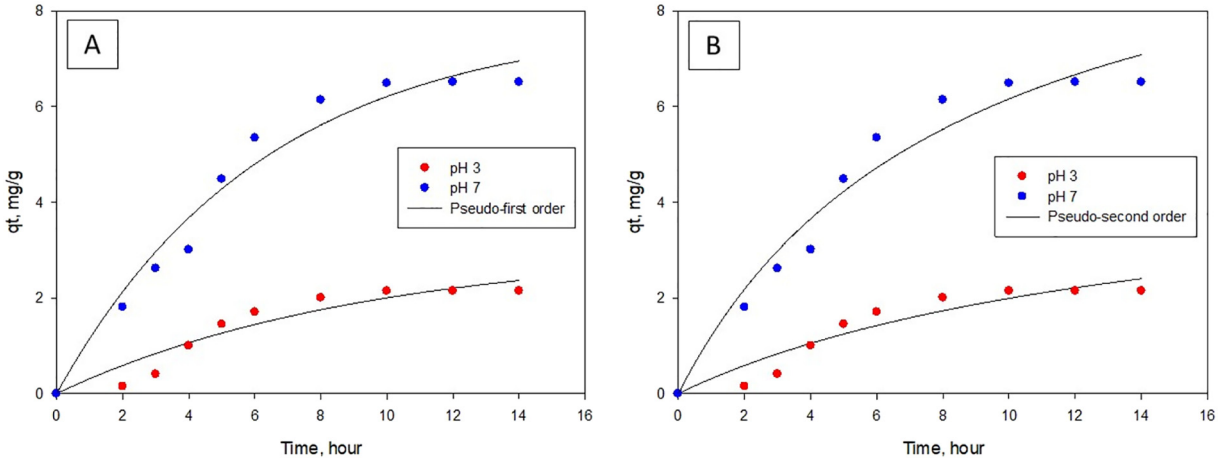

Fig. 5. Desorption kinetic of TET from 20N1R with (A) pseudo-first-order fitting and (B) pseudo-second-order fitting.

because at pH < 3.3, the TET molecules present as cations while the surface of 20N1R is negatively charged; there is an attractive electrostatic force between two different-charged molecules that constrain the desorption. At pH 7, TET molecules present as zwitterions, that the net charge of the entire molecule was zero. This results in the weakening of the electrostatic interaction between TET and 20N1R; hence, TET molecules can escape more easily.

4. Conclusion

Rarasaponin extracted from the *Sapindus rarak* plant has been successfully incorporated to modify the surface of nanocrystalline cellulose (NCC) particles. Rarasaponin-modified NCC possesses better adsorption ability towards tetracycline (TET) than that of unmodified NCC. Adsorption of the TET@NCC/Rara system proceeds endothermically, where a physisorption mechanism is dominant. Thermodynamic studies revealed that the presence of rarasaponin promotes the spontaneity of adsorption. The desorption kinetics of TET from NCC/Rara showed higher desorption efficiency at pH 7. TET loading onto NCC can be improved with such low rarasaponin concentration (0.5–1 μg/mL); at this concentration, good biocompatibility of rarasaponin (crude extract) can be expected.

CRediT authorship contribution statement

Vania Bundjaja: Investigation, Formal analysis, Writing - original draft. **Tirta Mutiara Sari:** Investigation, Formal analysis. **Felycia Edi Soetaredjo:** Funding acquisition. **Maria Yuliana:** Writing - review & editing. **Artik Elisa Angkawijaya:** Writing - original draft. **Suryadi Ismadji:** Funding acquisition. **Kuan-Chen Cheng:** Writing - review & editing. **Shella Permatasari Santoso:** Writing - original draft, Funding acquisition, Writing - review & editing.

Declaration of competing interest

The authors declare that they have no known competing financial interests or personal relationships that could have appeared to influence the work reported in this paper.

Acknowledgment

Financial support from the National Taiwan University of Science and Technology through the Joint Research Project is highly acknowledged.

Appendix A. Supplementary data

Supplementary data to this article can be found online at https://doi.org/10.1016/j.molliq.2019.112433.

References

[1] V. Andonova, Synthetic polymer-based nanoparticles: intelligent drug delivery systems, in: B. Reddy (Ed.), Acrylic Polymers in Healthcare, Intechopen, UK, 2017.
[2] W.H.D. Jong, P.J.A. Borm, Drug delivery and nanoparticles: applications and hazards, Int. J. Nanomedicine 3 (2008) 133–149.
[3] M.S.H. Akash, K. Rehman, S. Chen, Natural and synthetic polymers as drug carriers for delivery of therapeutic proteins, Polym. Rev. 55 (2015) 371–406.
[4] V.S.V. Priya, H. Roy, N. Jyothi, N.L. Prasanthi, Polymers in drug delivery technology, Types of Polymers and Applications 5 (2016) 305–308.
[5] J. Albers, K. Knop, P. Kleinebudde, Brand-to-brand and batch-to-batch uniformity of microcrystalline cellulose in direct tableting with a pneumohydraulic tablet press, Pharm. Ind. 68 (2006) 1420–1428.
[6] M.C. Gohel, R.K. Parikh, B.K. Brahmbhatt, A.R. Shah, Preparation and assessment of novel coprocessed superdisintegrant consisting of crospovidone and sodium starch glycolate: a technical note, AAPS Pharm. Sci. Tech. 8 (2007) E63–E69.
[7] J.K. Jackson, K. Letchford, B.Z. Wasserman, L. Ye, W.Y. Hamad, H.M. Burt, The use of nanocrystalline cellulose for the binding and controlled release of drugs, Int. J. Nanomedicine 6 (2011) 321.
[8] D. Plackett, K. Letchford, J. Jackson, H. Burt, A review of nanocellulose as a novel vehicle for drug delivery, Nord. Pulp Pap. Res. J. 29 (2014) 105–118.
[9] S.P. Santoso, L. Laysandra, J.N. Putro, J. Lie, F.E. Soetaredjo, S. Ismadji, A. Ayucitra, Y.-H. Ju, Preparation of nanocrystalline cellulose-montmorillonite composite via thermal radiation for liquid-phase adsorption, J. Mol. Liq. 233 (2017) 29–37.
[10] Y.K. Song, I.M.L. Chew, T.S.Y. Choong, K.W. Tan, NanoCrystalline Cellulose, an environmental friendly nanoparticle for pharmaceutical application–a quick study, MATEC Web of Conferences, EDP Sciences, 2016.
[11] G. Thoorens, F. Krier, B. Leclercq, B. Carlin, B. Evrard, Microcrystalline cellulose, a direct compression binder in a quality by design environment—a review, Int. J. Pharm. 473 (2014) 64–72.
[12] A. Kurniawan, H. Sutiono, N. Indraswati, S. Ismadji, Removal of basic dyes in binary system by adsorption using rarasaponin–bentonite: revisited of extended Langmuir model, Chem. Eng. J. 189 (2012) 264–274.
[13] A. Kurniawan, H. Sutiono, Y.-H. Ju, F.E. Soetaredjo, A. Ayucitra, A. Yudha, S. Ismadji, Utilization of rarasaponin natural surfactant for organo-bentonite preparation: application for methylene blue removal from aqueous effluent, Micropor. Mesopor. Mater. 142 (2011) 184–193.
[14] R.J. Farn, Chemistry and Technology of Surfactants, John Wiley & Sons, 2008.
[15] J.N. Putro, S. Ismadji, C. Gunarto, M. Yuliana, S.P. Santoso, F.E. Soetaredjo, Y.-H. Ju, The effect of surfactants modification on nanocrystalline cellulose for paclitaxel loading and release study, J. Mol. Liq. 282 (2019) 407–414.
[16] W. Qing, Y. Wang, Y. wang, D. Zhao, X. Liu, J. Zhu, The modified nanocrystalline cellulose for hydrophobic drug delivery, Appl. Surf. Sci. 366 (2016) 404–409.
[17] P.K. Rahman, E. Gakpe, Production, characterisation and applications of biosurfactants-review, Biotechnology 7 (2) (2008) 360–370, https://doi.org/10.3923/biotech.2008.360.370.
[18] I. Chopra, M. Roberts, Tetracycline antibiotics: mode of action, applications, molecular biology, and epidemiology of bacterial resistance, Microbiol. Mol. Biol. Rev. 65 (2001) 232–260.
[19] L. Jin, X. Amaya-Mazo, M.E. Apel, S.S. Sankisa, E. Johnson, M.A. Zbyszynska, A. Han, Ca^{2+} and Mg^{2+} bind tetracycline with distinct stoichiometries and linked deprotonation, Biophys. Chem. 128 (2007) 185–196.
[20] R.-A. Mitran, M. Deaconu, C. Matei, D. Berger, Mesoporous silica as carrier for drug-delivery systems, Nanocarriers for Drug Delivery, Elsevier 2019, pp. 351–374.
[21] N.D. Stebbins, M.A. Ouimet, K.E. Uhrich, Antibiotic-containing polymers for localized, sustained drug delivery, Adv. Drug Deliv. Rev. 78 (2014) 77–87.
[22] X.M. Dong, J.-F. Revol, D.G. Gray, Effect of microcrystallite preparation conditions on the formation of colloid crystals of cellulose, Cellulose 5 (1998) 19–32.
[23] S. Hiai, H. Oura, T. Nakajima, Color reaction of some sapogenins and saponins with vanillin sulfuric acid, Planta Med. 29 (1976) 116–122.
[24] C.J. Wijaya, S.N. Saputra, F.E. Soetaredjo, J.N. Putro, C.X. Lin, A. Kurniawan, Y.-H. Ju, S. Ismadji, Cellulose nanocrystals from passion fruit peels waste as antibiotic drug carrier, Carbohydr. Polym. 175 (2017) 370–376.
[25] Z. Hu, S. Ballinger, R. Pelton, E.D. Cranston, Surfactant-enhanced cellulose nanocrystal Pickering emulsions, J. Colloid Interface Sci. 439 (2015) 139–148.
[26] D. Roy, M. Semsarilar, J.T. Guthrie, S. Perrier, Cellulose modification by polymer grafting: a review, Chem. Soc. Rev. 38 (2009) 2046–2064.
[27] B.L. Tardy, S. Yokota, M. Ago, W. Xiang, T. Kondo, R. Bordes, O.J. Rojas, Nanocellulose–surfactant interactions, Curr. Opin. Colloid Interface Sci. 29 (2017) 57–67.
[28] M. Gorman, The evidence from infrared spectroscopy for hydrogen bonding: a case history of the correlation and interpretation of data, J. Chem. Educ. 34 (1957) 304.
[29] S. Park, J.O. Baker, M.E. Himmel, P.A. Parilla, D.K. Johnson, Cellulose crystallinity index: measurement techniques and their impact on interpreting cellulase performance, Biotechnol. Biofuels 3 (2010) 10.
[30] S.P. Santoso, A. Kurniawan, F.E. Soetaredjo, K.-C. Cheng, J.N. Putro, S. Ismadji, Y.-H. Ju, Eco-friendly cellulose–bentonite porous composite hydrogels for adsorptive removal of azo dye and soilless culture, Cellulose 26 (2019) 3339–3359.
[31] I. Langmuir, The constitution and fundamental properties of solids and liquids. Part I. Solids, J. Am. Chem. Soc. 38 (1916) 2221–2295.
[32] L. Laysandra, I.J. Ondang, Y.-H. Ju, B.H. Ariandini, A. Mariska, F.E. Soetaredjo, J.N. Putro, S.P. Santoso, F.L. Darsono, S. Ismadji, Highly adsorptive chitosan/saponin-bentonite composite film for removal of methyl orange and Cr(VI), Environ. Sci. Pollut. Res. 26 (2019) 5020–5037.
[33] H. Freundlich, Of the adsorption of gases. Section II. Kinetics and energetics of gas adsorption. Introductory paper to section II, T. Faraday Soc. 28 (1932) 195–201.
[34] D.D. Do, Adsorption Analysis: Equilibria and Kinetics, 2, Imperial college press, London, 1998.
[35] S. Lagergren, About the theory of so-called adsorption of soluble substances, K. Sven. Vetenskapsakad. Handl. 24 (1898) 1–39.
[36] W. Plazinski, W. Rudzinski, A. Plazinska, Theoretical models of sorption kinetics including a surface reaction mechanism: a review, Adv. Colloid Interf. Sci. 152 (2009) 2–13.
[37] A.V. Le, S.E. Parks, M.H. Nguyen, P.D. Roach, Improving the vanillin-sulphuric acid method for quantifying total saponins, Technologies 6 (2018) 84.
[38] I.-L. Shiau, T.-L. Shih, Y.-N. Wang, H.-T. Chen, Quantification for saponin from a soapberry (Sapindus mukorossi Gaertn) in cleaning products by a chromatographic and two colorimetric assays, J. Fac. Agr. Kyushu U. 54 (2009) 215–221.
[39] A.A. Karim, A. Azlan, Fruit pod extracts as a source of nutraceuticals and pharmaceuticals, Molecules 17 (2012) 11931–11946.
[40] S.S. Yudha, E. Angasa, R. Mariska, J. Hendri, Water extracts of Sapindus rarak as medium/reduction system for silver nanoparticles formation, Asian J. Chem. 25 (2013) 433–435.
[41] T. Morikawa, Y. Xie, K. Ninomiya, M. Okamoto, O. Muraoka, D. Yuan, M. Yoshikawa, T. Hayakawa, Inhibitory effects of acylated acyclic sesquiterpene oligoglycosides

from the pericarps of Sapindus rarak on tumor necrosis factor-alpha-induced cytotoxicity, Chem. Pharm. Bull. 58 (2010) 1276–1280.
[42] T. Faysoon, Molluscicidal Activity of Saponins From Sapindus Rarak Fruits on *Pomacea canaliculata*, Master Thesis Chulalongkorn University, 2006.
[43] J. Biggar, M. Cheung, Adsorption of picloram (4-amino-3, 5, 6-trichloropicolinic acid) on panoche, ephrata, and palouse soils: a thermodynamic approach to the adsorption mechanism 1, Soil Sci. Soc. Am. J. 37 (1973) 863–868.
[44] A.A. Khan, R. Singh, Adsorption thermodynamics of carbofuran on Sn (IV) arsenosilicate in H^+, Na^+ and Ca^{2+} forms, Colloid Surf 24 (1987) 33–42.
[45] A.W. Neto, T.N. Dentas, A.A.D. Neto, A. Gurgel, Recent advances on the use of surfactant systems as inhibitors of corrosion on metallic surfaces, in: M. Fanun (Ed.), The Role of Colloidal Systems in Environmental Protection, Elsevier BV, UK, 2014.